



## Observation of a Large Reaction Cross Section in the Drip-Line Nucleus $^{22}\text{C}$

K. Tanaka,<sup>1</sup> T. Yamaguchi,<sup>2</sup> T. Suzuki,<sup>2</sup> T. Ohtsubo,<sup>3</sup> M. Fukuda,<sup>4</sup> D. Nishimura,<sup>4</sup> M. Takechi,<sup>4,1</sup> K. Ogata,<sup>5</sup> A. Ozawa,<sup>6</sup>  
 T. Izumikawa,<sup>7</sup> T. Aiba,<sup>3</sup> N. Aoi,<sup>1</sup> H. Baba,<sup>1</sup> Y. Hashizume,<sup>6</sup> K. Inafuku,<sup>8</sup> N. Iwasa,<sup>8</sup> K. Kobayashi,<sup>2</sup> M. Komuro,<sup>2</sup>  
 Y. Kondo,<sup>9</sup> T. Kubo,<sup>1</sup> M. Kurokawa,<sup>1</sup> T. Matsuyama,<sup>3</sup> S. Michimasa,<sup>1,\*</sup> T. Motobayashi,<sup>1</sup> T. Nakabayashi,<sup>9</sup> S. Nakajima,<sup>2</sup>  
 T. Nakamura,<sup>9</sup> H. Sakurai,<sup>1</sup> R. Shinoda,<sup>2</sup> M. Shinohara,<sup>9</sup> H. Suzuki,<sup>10,6</sup> E. Takeshita,<sup>1,†</sup> S. Takeuchi,<sup>1</sup> Y. Togano,<sup>11</sup>  
 K. Yamada,<sup>1</sup> T. Yasuno,<sup>6</sup> and M. Yoshitake<sup>2</sup>

<sup>1</sup>RIKEN Nishina Center, Saitama 351-0198, Japan

<sup>2</sup>Department of Physics, Saitama University, Saitama 338-8570, Japan

<sup>3</sup>Department of Physics, Niigata University, Niigata 950-2181, Japan

<sup>4</sup>Department of Physics, Osaka University, Osaka 560-0043, Japan

<sup>5</sup>Department of Physics, Kyushu University, Fukuoka 812-8581, Japan

<sup>6</sup>Institute of Physics, University of Tsukuba, Ibaraki 305-8571, Japan

<sup>7</sup>Radio-Isotope Center, Niigata University, Niigata 951-8510, Japan

<sup>8</sup>Department of Physics, Tohoku University, Miyagi 980-8578, Japan

<sup>9</sup>Department of Physics, Tokyo Institute of Technology, Tokyo 152-8551, Japan

<sup>10</sup>Department of Physics, The University of Tokyo, Tokyo 113-0033, Japan

<sup>11</sup>Department of Physics, Rikkyo University, Tokyo 171-8501, Japan

(Received 28 October 2009; published 8 February 2010)

Reaction cross sections ( $\sigma_R$ ) for  $^{19}\text{C}$ ,  $^{20}\text{C}$  and the drip-line nucleus  $^{22}\text{C}$  on a liquid hydrogen target have been measured at around 40A MeV by a transmission method. A large enhancement of  $\sigma_R$  for  $^{22}\text{C}$  compared to those for neighboring C isotopes was observed. Using a finite-range Glauber calculation under an optical-limit approximation the rms matter radius of  $^{22}\text{C}$  was deduced to be  $5.4 \pm 0.9$  fm. It does not follow the systematic behavior of radii in carbon isotopes with  $N \leq 14$ , suggesting a neutron halo. It was found by an analysis based on a few-body Glauber calculation that the two-valence neutrons in  $^{22}\text{C}$  preferentially occupy the  $1s_{1/2}$  orbital.

DOI: 10.1103/PhysRevLett.104.062701

PACS numbers: 25.60.Dz, 21.10.Gv, 25.70.Mn, 27.30.+t

A nuclear halo is a structure with a dilute matter distribution which extends far beyond the core of the nucleus. In general terms, the halo may be regarded as a threshold phenomenon. A very loosely bound valence nucleon or nucleons held in a short-range potential well can tunnel into the surrounding space with significant probability to be found at distances much greater than the nuclear radius [1]. The development of the halo is related to the separation energy of the valence nucleon(s) and the reduced mass of the system [2] as well as the centrifugal barrier [3]. The original and most famous halo nuclide is  $^{11}\text{Li}$ . Its special spatial properties were discovered by Tanihata *et al.* in 1985 [4]. The nucleus has attracted much attention as a novel ‘‘Borromean’’ quantum three-body bound system, where its two-body subsystems, two neutrons and  $^{10}\text{Li}$ , are both unbound. A melting of the  $N = 8$  magic number, whereby the  $0p_{1/2}$  and  $1s_{1/2}$  orbitals are nearly degenerate, is suggested in  $^{11}\text{Li}$  [5,6].

$^{22}\text{C}$  is an intriguing nucleus, since its separation energy of two-valence neutrons ( $S_{2n}$ ), evaluated to be  $420 \pm 940$  keV, is comparable with that of  $^{11}\text{Li}$  ( $300 \pm 19$  keV) [7]. Particle instability of  $^{21}\text{C}$  [8] allows us to treat  $^{22}\text{C}$  as a Borromean nucleus. Furthermore,  $^{22}\text{C}$  has 16 neutrons, which corresponds to a new magic number [9,10] for neutron-rich nuclei. The appearance of the new magic

number is regarded as a natural consequence of the strong mixing between the  $0d_{5/2}$  and  $1s_{1/2}$  orbitals, leaving a large gap to the  $0d_{3/2}$  orbital. Thus, whether weakly bound neutrons in  $^{22}\text{C}$  occupy the  $1s_{1/2}$  or  $0d_{5/2}$  orbital is of crucial interest. However, little is known about  $^{22}\text{C}$  beyond its half life [11]. In this Letter, we report on new measurements of the reaction cross section ( $\sigma_R$ ) for  $^{19,20,22}\text{C}$  on a liquid hydrogen target at around 40A MeV incident energy made at the RIKEN projectile fragment separator (RIPS) [12], a part of the RI beam factory operated by RIKEN Nishina Center and CNS, the University of Tokyo.

The  $^{19,20,22}\text{C}$  beams were delivered from the RIPS, as follows. A 63A MeV  $^{40}\text{Ar}$  primary beam with an intensity of 100 pnA was bombarding a Ta ( $333 \text{ mg/cm}^2$ ) production target. A thin wedge-shaped Al degrader (average thickness of  $116 \text{ mg/cm}^2$  and average slope of 0.57 mrad) was placed at the first focal plane (F1) of the RIPS. The momentum acceptance of  $\pm 3\%$  for the secondary beam was defined by the slit at F1. The particle identification of the secondary beams was made event-by-event by measuring magnetic rigidity ( $B\rho$ ), time of flight (TOF) between the second (F2) and the third (F3) focal planes of the RIPS, and energy loss ( $\Delta E$ ) of each nucleus. The intensities of the  $^{19}\text{C}$ ,  $^{20}\text{C}$  and  $^{22}\text{C}$  beams were  $1.8 \times 10^4$ ,  $1.8 \times 10^3$  and 10 counts per hour, respectively.

The secondary beams bombarded a 204 mg/cm<sup>2</sup> thick liquid hydrogen cell, a part of the “cryogenic proton and alpha target system” (CRYPTA) [13], located at F3. The entrance and exit windows were 11 mg/cm<sup>2</sup> thick havar foils with a diameter of 40 mm. The proton target provides a larger reaction rate of  $\sim 7.0\%$  for the same energy loss of the <sup>22</sup>C beam in both target materials than the  $\sim 2.5\%$  of the carbon often used in our previous experiments [9,14]. The uniformity in the thickness of this target over the whole area was maintained at better than 2% during the measurement by controlling the temperature ( $15.9 \pm 0.2$  K) [15] of the system. The energies of <sup>19</sup>C, <sup>20</sup>C and <sup>22</sup>C at the midpoint of the reaction target were 40, 40, and 41 MeV/nucleon, respectively. The beam position at the reaction target was measured by parallel-plate avalanche counters (PPACs).

The noninteracting C nuclei in the target were transported by a superconducting triplet quadrupole (STQ) magnet [16] to the final focal plane (F4) of the RIPS, located 5 m downstream of the reaction target. We used an experimental setup (“the TOF mass analyzer for RI beam experiments” -TOMBEE) similar to that described in Refs. [17,18]. Particles were tracked by PPACs and identified using a large area Si-NaI telescope (two layers of circular Si detector with size of 123 mm $\phi$   $\times$  320  $\mu$ m, and NaI of 5'' $\phi$   $\times$  6 cm) thus providing a measurement of interaction cross sections ( $\sigma_I$ ) by the transmission method. The nuclear charge ( $Z$ ) and mass ( $A$ ) resolutions in FWHM were found to be  $\Delta Z/Z \sim 4.0\%$ , 1.3% and  $\Delta A/A \sim 0.6\%$ , 2.2% in front of and behind the reaction target, respectively. These resolutions were sufficient to unambiguously

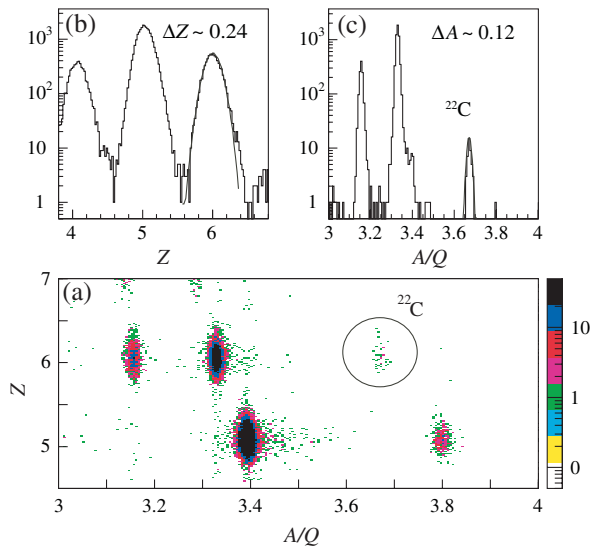


FIG. 1 (color). (a) Two-dimensional plot of  $Z$  versus  $A/Q$  in front of the reaction target. (b)  $Z$  projection of Fig. 1(a). The solid line indicates a Gaussian fit to the  $Z = 6$  peak, yielding a  $\Delta Z = 0.24$  in FWHM. (c)  $A/Q$ -projection spectrum for the  $Z = 6$  particles. The solid line indicates a Gaussian fit to the <sup>22</sup>C peak, yielding a  $\Delta A = 0.12$  in FWHM.

identify the  $Z$  and  $A$  for each beam particle as shown in Fig. 1.

The  $\sigma_I$  was obtained by the equation  $\sigma_I = (-1/N_I) \times \ln(\Gamma/\Gamma_0)$ , where  $\Gamma$  is the ratio of the number of noninteracting nuclei to that of incident nuclei for a target-in-measurement and  $\Gamma_0$  is the same ratio for an empty-target measurement. The number of target nuclei per unit area is denoted as  $N_I$ . The values of  $\Gamma_0$  were greater than 0.95 and those of  $\Gamma$  were 0.80–0.89. The deviation of  $\Gamma_0$  from unity was mainly due to nuclear interactions in the detectors. The momentum and angular emittance guaranteed full transmission in the STQ section for noninteracting C particles. This was studied using the simulation code MOCADI [19], which took into account the effect of fragmentations and small-angle deflections due to multiple-Coulomb scattering in the reaction target. In practice, it was achieved by restricting the beam angle and position at the target ( $\theta$ ,  $\phi \leq \pm 30$  mrad,  $r \leq 17$  mm) in an offline analysis by ray tracing with the PPACs located at F3.

The error bars of  $\sigma_I$  for <sup>19,20</sup>C are found to be comparable to the inelastic scattering cross sections ( $\sigma_{\text{inel.}}$ ) of <sup>19,20</sup>C +  $p$  reactions, reported in Refs. [20,21], where  $\gamma$ -ray spectroscopy experiments at around 40–50A MeV were performed. We assumed <sup>22</sup>C has no excited states, and therefore we approximated  $\sigma_R \approx \sigma_I$ . The  $\sigma_R$  determined in this way are listed in Table I, together with predictions of  $\sigma_R$  by a Glauber calculation [22], which is an established scattering theory based on the eikonal and the adiabatic approximations.

The Glauber calculation is based on the few-body (FB) approach assuming a one-neutron halo structure for <sup>19</sup>C and the optical-limit (OL) approach for <sup>20</sup>C. The experimental values of  $\sigma_R$  for <sup>19,20</sup>C are consistent with the predictions as seen in Table I. We observed a large enhancement in  $\sigma_R$  for <sup>22</sup>C compared to <sup>19,20</sup>C, albeit with rather large uncertainty (20%). This enhancement is not reproduced by a calculation using the same FB approach assuming a pure  $s$ -wave two-neutron halo structure [22]. This may be due to a smaller  $S_{2n}$  than that assumed in the calculation. The large  $\sigma_R$  suggests a neutron halo structure in <sup>22</sup>C.

The rms matter radius ( $\tilde{r}_m \equiv \langle r_m^2 \rangle^{1/2}$ ) was extracted using the Glauber model. In the OL approach with the finite-range treatment that we adopted [23], the beam energy ( $E$ ) dependence of  $\sigma_R$  for the <sup>12</sup>C + <sup>12</sup>C system is well described for  $E = 30A$ – $1000A$  MeV. To calculate  $\sigma_R$  we assumed a density distribution ( $\rho(r)$ ) of <sup>22</sup>C to be a harmonic oscillator (HO) function [24] for the core (<sup>20</sup>C)

TABLE I. Reaction cross sections ( $\sigma_R$ ) in millibarns.

| $A$ | $\sigma_R$ | $\sigma_R^{\text{calc.}}$ [22] |
|-----|------------|--------------------------------|
| 19  | 754(22)    | 758                            |
| 20  | 791(34)    | 761                            |
| 22  | 1338(274)  | $\geq 957$                     |

plus the square of the Yukawa function for the two-valence neutrons.

The square of the Yukawa function is known to be a good approximation to the shape of a single-particle density at the outer region of a core with centrifugal barriers. The assumed density is expressed as

$$\rho_p(r) = \text{HO}, \quad \rho_n(r) = \begin{cases} \text{HO} & (r \leq r_c) \\ \rho_0 \exp(-\lambda r)/r^2 & (r > r_c), \end{cases} \quad (1)$$

where  $r_c$  is the critical radius at which the HO function crosses with the square of the Yukawa function and  $\lambda$  is the asymptotic slope of the tail,  $\lambda = 2\sqrt{2}\mu\epsilon/\hbar$ , where  $\mu$  denotes the reduced mass of a single neutron and  $^{20}\text{C}$ . We fixed  $\epsilon$  to be  $S_{2n}/2 = 210$  keV, or  $S_n = 750$  keV [7]. The width parameter ( $a_{\text{HO}}$ ) of the core, chosen to be 2.22 fm so as to reproduce the present  $\sigma_R$  data of  $^{20}\text{C} + p$ , is common to both protons and neutrons. The  $r_c$  value was used as a parameter. The resultant  $\tilde{r}_m$  value with  $\epsilon = S_{2n}/2$  was  $5.4 \pm 0.9$  fm for  $r_c = 5.39$  fm and that with  $\epsilon = S_n$  was  $5.0 \pm 0.8$  fm for  $r_c = 3.90$  fm, respectively, so as to reproduce the present  $\sigma_R$  data of  $^{22}\text{C} + p$ . It should be noted that both results overlap within their error bars. The result is displayed in Fig. 2. It can be seen that the  $\tilde{r}_m$  of  $^{22}\text{C}$  does not follow the systematic behavior of radii in carbon isotopes with  $N \leq 14$ , suggesting a neutron halo.

We may not exclude the possibility that the large  $\sigma_R$  and the radius of 5.4 fm are due to a deformation effect. According to the ‘‘pairing-plus-quadrupole’’ model [25], where the nuclear shapes are parameterized as rotational ellipsoids with the deformation limited to the quadrupole contribution, the spherical part of the nuclear radius ( $\tilde{r}_m^{\text{sph.}}$ ) is increased by a factor of  $\sqrt{1 + \frac{5}{4\pi}\beta_2^2}$ . If the moderate

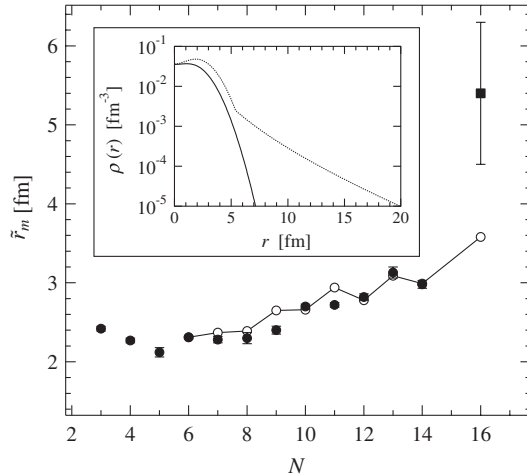


FIG. 2. The  $\tilde{r}_m$  as a function of the neutron number of C isotopes. The filled square and circles show the present result and those determined at GSI [14], respectively, while open symbols are the result of the calculation [22]. The lines connect the open circles. The inset shows  $\rho_p(r)$  (solid line) and  $\rho_n(r)$  (dotted line) of  $^{22}\text{C}$  for the determined parameter. See text.

deformation of  $\beta_2 \sim -0.258$  predicted by the deformed Skyrme Hartree-Fock model [26] is used, the increase is only 1.3%. Hence it seems that the large radius is probably not due to a deformation effect.

We then studied whether the configuration of two-valence neutrons is  $(0d_{5/2})_{J=0}^2$  or  $(1s_{1/2})_{J=0}^2$ , i.e.,  $\varphi(\mathbf{r}_1, \mathbf{r}_2) = [\phi_j(\mathbf{r}_1)\phi_j(\mathbf{r}_2)]_{J=0}$ , where  $j = 0d_{5/2}$  or  $1s_{1/2}$ . We calculated  $\sigma_R$  with the FB approach under the finite-range treatment as a function of the  $s$ -wave spectroscopic factor  $f$  (the relative ratio of the wave function of  $(0d_{5/2})_{J=0}^2$  or  $(1s_{1/2})_{J=0}^2$ ) in the following expression:

$$\varphi(\mathbf{r}_1, \mathbf{r}_2) = \{\sqrt{f}[\phi_{1s_{1/2}}(\mathbf{r}_1)\phi_{1s_{1/2}}(\mathbf{r}_2)]_{J=0} + \sqrt{1-f}[\phi_{0d_{5/2}}(\mathbf{r}_1)\phi_{0d_{5/2}}(\mathbf{r}_2)]_{J=0}\}. \quad (2)$$

In the analysis, each wave function  $\phi_{0d_{5/2}}(\mathbf{r})$  and  $\phi_{1s_{1/2}}(\mathbf{r})$  was obtained by solving the Schrödinger equation in a Woods-Saxon potential for a given value of  $S_{2n}/2$ , with a diffuseness parameter of 0.6 fm and a radius parameter of  $1.2A^{1/3}$  fm. As for the core of  $^{20}\text{C}$ , we took the HO density distribution with  $a_{\text{HO}} = 2.22$  fm for both protons and neutrons.

In Fig. 3,  $\sigma_R$  for  $f = 1.0$  and that for  $f = 0.0$  are plotted, for two different values of  $S_{2n}$ . It can be seen from the figure that the discrepancy between the measured  $\sigma_R$  and calculated  $\sigma_R$  for  $f = 0.0$  is much larger than that for  $f = 1.0$  with  $S_{2n} = 420$  keV (dashed lines). It decreases if we take  $S_{2n} = 10$  keV instead (solid lines). The pure  $1s_{1/2}$  wave function ( $f = 1.0$ ) with  $S_{2n} = 10$  keV reproduced the measured  $\sigma_R$  for  $^{22}\text{C}$  within the error bar of the experimental value. This indicates that two-valence neutrons in  $^{22}\text{C}$  preferentially occupy the  $1s_{1/2}$  orbital. The  $s$ -wave dominance is consistent with a theo-

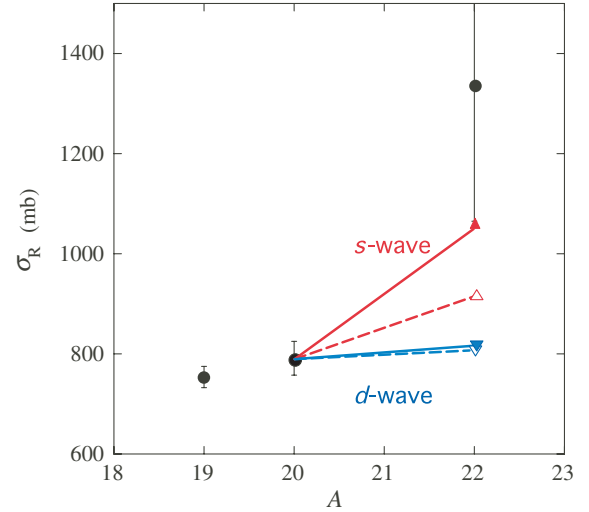


FIG. 3 (color). The  $\sigma_R$  for  $f = 1.0$  (red triangles) and that for  $f = 0.0$  (blue triangles), with  $S_{2n} = 420$  keV (open symbols) and  $S_{2n} = 10$  keV (closed symbols), respectively. The lines are to guide the eye. The experimental data (solid circles) as a function of the mass number of C isotopes are also plotted.

retical prediction [27]. It also indicates that a small  $S_{2n}$  is necessary to account for the observed large  $\sigma_R$ .

Another possibility for the large  $\sigma_R$  may be a core perturbation. Ref. [28] reports the charge radius of  $^{11}\text{Li}$  is larger than that of  $^9\text{Li}$  by approximately 0.25 fm. This indicates that the inert core  $^9\text{Li}$  in  $^{11}\text{Li}$  is significantly perturbed. We calculated  $\sigma_R$  assuming the perturbed core increased by 0.25 fm, i.e.  $a_{\text{HO}} = 2.47 (= 2.22 + 0.25)$  fm. With the same FB approach described above, the  $\sigma_R$  value for  $f = 1.0$  with  $S_{2n} = 420$  keV is obtained to be 1110 mb and lies within the error bar, while that for  $f = 0.0$  with  $S_{2n} = 420$  keV is only 860 mb. It should be noted that the  $\sigma_R$  value for  $f = 0.0$  with  $S_{2n} = 10$  keV is 880 mb. These results indicate that the  $s$ -wave dominance for the two-valence neutrons is necessary even for the case of the perturbed core.

It should be noted that the validity of the Glauber model at 40A MeV is questioned in Ref. [22]. Therefore we examined its accuracy, in particular, for the eikonal approximation used, by calculating  $\sigma_R$  quantum mechanically. We adopted a microscopic folding model [29] using the  $\rho_p(r)$  and  $\rho_n(r)$  obtained via our Glauber analysis, shown in the inset of Fig. 2, as input. For the effective nucleon-nucleon interaction we adopted the  $g$  matrix based on the Bonn-B potential [30], obtained by the Melbourne group [31]. Only the central part of the microscopic optical potential between  $p$  and  $^{22}\text{C}$  was evaluated. The resultant value of  $\sigma_R$  was 1321 mb, which reproduced very well the experimental value of  $1338 \pm 274$  mb. The microscopic folding model calculation contains no free parameters. Thus, the good agreement between the microscopic folding model calculation using the results of the Glauber analysis and the experimental result guarantees, at least to some extent, the validity of our Glauber analysis at around 40A MeV. More detailed analysis explicitly including the breakup states of  $^{22}\text{C}$  will still be important to draw a more definite conclusion on the structure of  $^{22}\text{C}$ .

In summary, this Letter reports the first measurement of reaction cross sections for  $^{19,20,22}\text{C} + p$  reactions. The observed reaction cross section for  $^{22}\text{C}$  is significantly larger than those for  $^{19,20}\text{C}$ . Using a finite-range Glauber calculation under an optical-limit approximation, the rms matter radius of  $^{22}\text{C}$  was deduced to be  $5.4 \pm 0.9$  fm. It does not follow the systematic behavior of radii in carbon isotopes with  $N \leq 14$ , suggestive of a neutron halo. The configuration of two-valence neutrons in  $^{22}\text{C}$  was studied via a finite-range few-body Glauber calculation. It was found that two-valence neutrons favor occupation of the  $1s_{1/2}$  orbital. A small separation energy of two-valence neutrons and/or a core perturbation is suggested to account for the large reaction cross section. It is important to measure the reaction cross section for  $^{22}\text{C}$  on other nuclei and/or at higher beam energy with higher accuracy in order to determine the density distribution and to establish the halo structure experimentally.

The authors gratefully acknowledge all of the staff at the RIKEN ring cyclotron for their stable operation of the accelerator during the experiment. We thank Dr. J. Miller at LBNL for his careful reading of the manuscript.

\*Present address: Center for Nuclear Study, The University of Tokyo, RIKEN campus, Saitama 351-0198, Japan.

†Present address: National Institute of Radiological Sciences, Chiba, 263-8555, Japan.

- [1] P.G. Hansen, A.S. Jensen, and B. Jonson, *Annu. Rev. Nucl. Sci.* **45**, 591 (1995).
- [2] P.G. Hansen and B. Jonson, *Europhys. Lett.* **4**, 409 (1987).
- [3] K. Riisager, A.S. Jensen, and P. Møller, *Nucl. Phys.* **A548**, 393 (1992).
- [4] I. Tanihata *et al.*, *Phys. Rev. Lett.* **55**, 2676 (1985).
- [5] H. Simon *et al.*, *Phys. Rev. Lett.* **83**, 496 (1999).
- [6] N. Aoi *et al.*, *Nucl. Phys.* **A616**, 181 (1997).
- [7] G. Audi, A.H. Wapstra, and C. Thibault, *Nucl. Phys.* **A729**, 337 (2003).
- [8] M. Langevin *et al.*, *Phys. Lett. B* **150**, 71 (1985).
- [9] A. Ozawa *et al.*, *Phys. Rev. Lett.* **84**, 5493 (2000).
- [10] R. Kanungo *et al.*, *Phys. Rev. Lett.* **102**, 152501 (2009).
- [11] K. Yoneda *et al.*, *Phys. Rev. C* **67**, 014316 (2003).
- [12] T. Kubo *et al.*, *Nucl. Instrum. Methods Phys. Res., Sect. B* **70**, 309 (1992).
- [13] H. Ryuto *et al.*, *Nucl. Instrum. Methods Phys. Res., Sect. A* **555**, 1 (2005).
- [14] A. Ozawa *et al.*, *Nucl. Phys.* **A691**, 599 (2001).
- [15] K. Tanaka *et al.*, *RIKEN Accel. Prog. Rep.* **40**, 20 (2007).
- [16] K. Kusaka *et al.*, *IEEE Trans. Appl. Supercond.* **14**, 310 (2004).
- [17] S. Takeuchi *et al.*, *Phys. Rev. C* **79**, 054319 (2009).
- [18] N. Aoi *et al.*, *Phys. Rev. Lett.* **102**, 012502 (2009).
- [19] N. Iwasa *et al.*, *Nucl. Instrum. Methods Phys. Res., Sect. B* **126**, 284 (1997).
- [20] Z. Elekes *et al.*, *Phys. Lett. B* **614**, 174 (2005).
- [21] Z. Elekes *et al.*, *Phys. Rev. C* **79**, 011302 (2009).
- [22] B. Abu-Ibrahim, W. Horiuchi, A. Kohama, and Y. Suzuki, *Phys. Rev. C* **77**, 034607 (2008).
- [23] Y. Yamaguchi *et al.*, *Phys. Rev. C* **70**, 054320 (2004).
- [24] B. Abu-Ibrahim, S. Iwasaki, W. Horiuchi, A. Kohama, and Y. Suzuki, *J. Phys. Soc. Jpn.* **78**, 044201 (2009).
- [25] B. S. Reehal and R. A. Sorensen, *Nucl. Phys.* **A161**, 385 (1971).
- [26] H. Sagawa, X. R. Zhou, X. Z. Zhang, and T. Suzuki, *Phys. Rev. C* **70**, 054316 (2004).
- [27] W. Horiuchi and Y. Suzuki, *Phys. Rev. C* **74**, 034311 (2006).
- [28] R. Sánchez *et al.*, *Phys. Rev. Lett.* **96**, 033002 (2006).
- [29] F. A. Brieva and J. R. Rook, *Nucl. Phys.* **A291**, 317 (1977).
- [30] R. Machleidt, K. Holinde, and Ch. Elster, *Phys. Rep.* **149**, 1 (1987).
- [31] K. Amos, P.J. Dortmans, H.V. von Geramb, S. Karataglidis, and J. Raynal, *Advances in Nuclear Physics*, edited by J. W. Negele and E. Vogt (Plenum, New York, 2000), Vol. 25, p. 275.